CHALMERS
UNIVERSITY OF TECHNOLOGY

UNIVERSITY OF GOTHENBURG

Serial synchrotron crystallography in drug discovery

Using on-chip co-crystallization on silicon nitride membranes

Master's thesis in Biotechnology

GABRIELLE WEHLANDER

Department of Biology and Biological Engineering
Chalmers University of Technology
Gothenburg, Sweden 2022
www.chalmers.com

Serial synchrotron crystallography in drug discovery

Using on-chip co-crystallization on silicon nitride membranes

GABRIELLE WEHLANDER

Department of Biology and Biological Engineering
Chalmers University of Technology

In collaboration with

Department of Chemistry and Molecular Biology
University of Gothernburg
Gothenburg, Sweden 2022

Serial synchrotron crystallography in drug discovery
Using on-chip co-crystallization on silicon nitride membranes

GABRIELLE WEHLANDER

Supervisors:
Gisela Brändén
Senior Lecturer at the Department of Chemistry and Molecular Biology, University of Gothenburg

Andreas Dunge
PhD student at the Department of Chemistry and Molecular Biology, University of Gothenburg and R&D, Discovery Science, Mechanistic and Structural Biology, AstraZeneca

Examiner:
Johan Larsbrink
Associate Professor at the Department of Biology and Biological Engineering, Industrial Biotechnology, Chalmers University of Technology

Department Biology and Biological Engineering
Chalmers University of Technology
SE-412 96 Gothenburg
Sweden
Phone: + 46 (0)31-772 10 00

Gothenburg, Sweden 2022

Acknowledgements

First of all, I want to thank my supervisors Gisela Brändén and Andreas Dunge from the University of Gothenburg, for giving me the opportunity to conduct a very interesting project. I also want to thank them for all guidance and support throughout the course of the project. Furthermore, I want to thank the employees at the Lundberg Laboratory for being welcoming and helpful. It has been a semester full of experiences and I'm truly thankful for having the possibility of learning a lot in a field highly relevant in drug development research.

Gabrielle Wehlander
June 26, 2022
Gothenburg

Abstract

Background: Serial synchrotron crystallography (SSX) has reached an increased popularity over the last years, predominantly thanks to its potential to derive room-temperature (RT) structures of proteins, with a low risk of causing radiation damages. Structure determination of ligand bound protein complexes is of major importance in today's drug development research, of which structure-based design is an important part. However, efficient methods for producing such samples, suitable for SSX, has not yet been established. It is therefore of uttermost importance to evaluate methods to efficiently produce protein-ligand complex crystals, to allow for high-scale implementation of SSX in the drug industry. One such method with promising potential is to perform on-chip co-crystallization of protein-ligand bound complexes on fixed-target sample delivery supports. By introducing the ligand by drying it on the supports further opens the possibilities of automating parts of the sample production.

Aim: The aim of the project was to i) evaluate the potential of performing on-chip crystallization on silicon nitride membranes, used as fixed-target supports at the MAX IV Laboratory, and ii) to evaluate the capability of two different co-crystallization techniques combined with on-chip crystallization.

Method: The protein soluble epoxide hydrolase was used as a proof-of-concept protein to evaluate on-chip co-crystallization on the silicon nitride membranes. The two co-crystallization techniques tested were i) to incubate protein and ligand in solution prior to crystallization, and ii) to dry ligand on the membranes, followed by adding protein crystallization drops. The capability of the two techniques was validated with RT-SSX at BioMAX, MAX IV.

Results: On-chip co-crystallization on the silicon nitride membranes was shown to be both possible and to generate well-diffracting crystals for RT-SSX. Structure analysis of the RT-SSX collected data showed that both co-crystallization techniques generated ligand bound protein complexes.

Discussion: The successful application of on-chip co-crystallization on the membranes makes it of highest interest to further evaluate the method using other proteins and ligands, to evaluate the possibility of implementing the method in the drug industry.

Key words: Room-temperature serial synchrotron crystallography, fixed-target sample delivery, on-chip crystallization, co-crystallization, soluble epoxide hydrolase, silicon nitride membranes

Contents

1 Introduction **1**

1.1 Background . . . 3

1.1.1 Protein crystals . . . 3

1.1.2 Protein crystallization . . . 7

1.1.3 Room-temperature serial synchrotron crystallography . . . 10

1.2 Aim . . . 12

2 Materials and metods **13**

2.1 Protein crystallization drop constituents and materials . . . 13

2.1.1 Protein . . . 13

2.1.2 Ligands . . . 13

2.1.3 Precipitants . . . 13

2.1.4 Seed . . . 14

2.1.5 Crystallization plates and fixed-target supports . . . 14

2.2 Screening of protein crystallization conditions . . . 14

2.2.1 Production of sEH microcrystals . . . 14

2.2.2 Co-crystallization . . . 15

2.2.3 On-chip crystallization . . . 16

2.3 RT-SSX at BioMAX . . . 16

2.3.1 Samples . . . 16

2.3.2 Data collection and processing . . . 17

3 Results **18**

3.1 Characteristics of crystals grown under different conditions . . . 18

3.1.1 The effect of drop ratio and seed dilution on the number and size of crystals 18

3.1.2 The capability of different ligands to be used for co-crystallization with sEH 19

3.1.3 On-chip crystallization . . . 22

3.2 RT-structures of the sEH-6N4 complex solved from the dry- and solution-co-crystallization samples . . . 22

3.2.1 Differences between the structures of the dry- and solution-co-crystallization samples . . . 23

3.2.2 Comparison of RT- and cryo-structures of the sEH-6N4 complex 25

4 Discussion **27**

5 Conclusion **30**

A Production of macrocrystals used to produce seed **33**

B Fixed-target sample introduction at BioMAX **34**

C Drop ratio screening **35**

D Position of residue Phe497 **36**

Abbreviations

DMSO: Dimethyl sulfoxide

PEG: Polyethylene glycol

PDB: Protein Data Bank

RT: Room temperature

sEH: Soluble epoxide hydrolase

SSX: Serial synchrotron crystallogaphy

SX: Serial crystallogaphy

XFEL: X-ray free electron laser

PDB association codes

1P8: 6-bromo-1,3-dihydro-2H-indol-2-one

5akj: Ligand 6N4 complex structure of soluble epoxide hydrolase solved at 100K

5akk: Ligand 1P8 complex structure of soluble epoxide hydrolase solved at 100K

5ald: Ligand FCW complex structure of soluble epoxide hydrolase solved at 100K

6N4: 2-(1H-benzimidazol-2-ylsulfanyl)ethanol

FCW: 5-cyclohexyl-1,3-dihydroindol-2-one

1. Introduction

Knowledge of the structure of proteins has a significant importance in several fields of biology and biotechnology, not least in drug discovery and development. Knowing the structure of a protein can be of help for understanding the function and dynamics of the molecule. Furthermore, it's crucial when it comes to determining the molecular interactions involved when a protein molecule binds to other molecules, for example drugs (1).

Over the years, X-ray crystallography has been the far most common method for determining macromolecular structures. By mid 2022, more than 190 000 structures had been deposited in the Protein Data Bank (PDB), whereof about 87.0% of the structures had been solved by X-ray crystallography (2). In addition to X-ray crystallography, nuclear magnetic resonance (NMR) and electron microscopy (EM) are commonly used methods, whereof EM has raised the most in popularity over the last five years. However, X-ray crystallography is by far still the most common method of use today and 73.6% of the structures reported to PDB in 2021 were solved by X-ray crystallography (2).

Structure determination using X-ray crystallography is based on illuminating a crystal of highly arranged molecules with X-rays (3), Figure 1.2(a). As the X-rays hit the crystal, they will diffract in different directions. The diffracted X-rays are detected as a diffraction pattern on a detector. The structure of the molecule constructing the crystal can then be derived from the diffraction patterns, using advanced algorithms.

In the field of protein crystallography, the conventional method has been to use one or a few large (>100µm), cryo-cooled protein crystals to collect a complete data set necessary solve the protein structure (4). However, over the last years the novel method serial crystallography (SX) has been developed and raised in popularity as it can be performed at room-temperature (RT) by using thousands of micrometre-sized crystals (microcrystals), where each crystal gives rise to one diffraction image. Determination of RT protein structures gives a more reliable view of the physiological structure, as cryo-cooling might induce structural changes to physiological important parts of the protein (4). Additionally, RT-measurements eliminates the need of cryo-protectants

needed when the crystals are cryo-cooled. Furthermore, the fact that the method utilizes small crystals also makes it well suited for proteins that are difficult to grow large crystals from. Thanks to this, structural determination of several membrane proteins has been made possible (5; 6).

SX can be performed at the two X-ray generating facilities X-ray free electron lasers (XFELs) and synchrotrons, where the microcrystals are introduced to the X-ray beam using either injection or fixed-target sample delivery techniques (7). Of the two techniques, fixed-target sample delivery has the potential of lowering the crystal handling steps by growing crystals directly on the fixed-target supports (on-chip crystallization). As protein crystals are fragile, this technique is of particular interest. However, in many labs, microcrystals are grown elsewhere and loaded to the supports (off-chip crystallization) (8), exposing the crystals for stress that might cause damages as well as increasing the labor intensity. It is hence of interest to investigate and develop different techniques for performing on-chip crystallization on different fixed-target supports to lower the crystal handling steps.

A further application of on-chip crystallization to make it of particular interest for the drug industry, is to grow ligand bound protein complex crystals directly on the supports. The two main techniques to produce crystals of protein-ligand complexes are soaking and co-crystallization. There are fixed-target supports specifically developed to be used with soaking (9). However, using soaking, modifications of already grown protein crystals are made, which might cause damages of the crystals (1). On the other hand, co-crystallization of protein with ligand allows for formation of the complex structure directly when the crystals are grown, eliminating the need of any post-crystallization modifications. Development of efficient co-crystallization techniques to be used with on-chip crystallization are of significant interest as it would lower the crystal handling steps when producing samples for SX. Furthermore, methods with a potential to be automated are of particular interest. One such co-crystallization method is to dry ligand on fixed-target supports prior to adding protein crystallization drops (dry-co-crystallization) (10).

In this project, serial synchrotron crystallography (SSX) at the beamline BioMAX, at the MAX IV Laboratory in Lund, was used to evaluate the possibilities of performing on-chip co-crystallization on the fixed-target supports standard silicon nitride membranes (Silson, UK). The protein soluble epoxide hydrolase (sEH) was used as a proof-of-concept protein as i) it has been successfully analyzed with RT-SSX for crystals grown off-chip and loaded on the membranes (Dunge *et al.*, in preparation), and ii) there is a large data bank of cryo-structures of the protein in complexes with different ligands (1). Co-crystallization was performed with three of these ligands,

whereof co-crystals of one of these were analyzed at BioMAX. Co-crystallization was performed with two techniques, the dry-co-crystallization technique and to incubate protein and ligand in solution prior to setting up crystallization drops (solution-co-crystallization). Furthermore, the RT-structures from samples produced with the two co-crystallization techniques were compared to the cryo-structure to identify any structural differences between the two temperatures.

1.1 Background

1.1.1 Protein crystals

Proteins can in similarity to many other molecules form crystals when solidifying. However, very specific conditions are needed, individual for each protein. Different proteins crystallize into different shapes, and a single protein can in some cases form more than one type of crystal (3). During crystallization, the protein molecules arranges themselves in a highly ordered three-dimensional array, where the molecules adopt only one or a few orientations.

An important component of protein crystals is water. Protein crystals contain both ordered and disordered water, where ordered water is predominantly found within the folded protein and in direct contact with the protein surface, whereas disordered water predominantly occupies spaces between the protein molecules (3). The ordered water molecules are located at the same positions in all protein molecules in the crystal, making it possible to localize their position while deriving the protein structure. Disordered water is on the other hand located differently around each protein and their specific locations can therefore not be derived. Both types of water are essential for the crystal and the crystals are destroyed if they dehydrate. It's therefore important to keep the crystals hydrated during a crystallography experiment, which can be done by keeping them in a solution or a humid atmosphere.

An important notification about protein crystals is that the protein structure is, with some exceptions, the same in the crystal as in solution (3). Proteins showing different shapes in the crystalline and solution states are rare. A further important notification to be aware of is that crystals of proteins are fragile. They are held together by weak forces, mainly by hydrogen bonds, which makes them much more fragile than inorganic molecules that are held together by electrostatic interactions (3). Protein crystals must therefore be handled with gentle techniques.

One way of describing a crystal is to identify the smallest volume that through multiplication can construct the whole crystal (3). This small volume is called a unit cell and is described by three

edges, **a**, **b** and **c**, of lengths a, b and c, and which are connected to each other with the angles α, β and γ, Figure 1.1(a). Depending on the internal structure of the unit cell, it can further be described by a specific space group. The space group contains information about lattice type and symmetry operations related to the unit cell. The lattice type describes the molecular positions, illustrated as lattice points, within a crystal lattice, which is formed when multiple unit cells are stacked together, 1.1(b). The symmetry operations refers to a set of operations that can be performed on the asymmetric unit of the unit cell, in order to construct the whole cell. The asymmetric unit is the smallest part of the unit cell able to construct the whole cell through the symmetry operations.

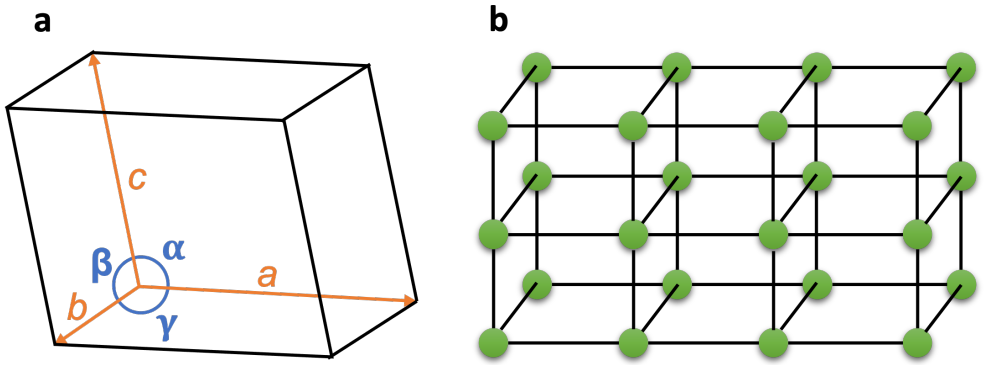

Figure 1.1: (a) A unit cell with edges of lengths a, b and c, which are connected with angles α, β and γ. (b) A crystal lattice created of unit cells stacked together. The green dots represent the lattice points.

Crystal diffraction

A typical crystallography experiment is performed by illuminating a crystal with X-rays, collect diffraction data and use mathematical operations to solve the protein structure (3), Figure 1.2(a). When the X-rays hit the crystal, the source X-ray beam is diffracted into many discrete X-ray beams. The diffracted beams can be regarded as reflections against a set of parallel planes in the crystal lattice, where each plane intersect the lattice points and where all planes are separated by a distance d, Figure 1.2(b). When incoming X-rays of wavelength λ are reflected on the planes with an angle θ, such that the condition in equation 1.1 is met, the diffracted beams will interfere constructively to produce a strong diffracted beam. The equation describing the relation between the wavelength and scattering angle is referred to as Bragg's law, where n is a positive integer. The intensity and direction of the diffracted beams are detected as a reflections on the detector.

$$n\lambda = 2dsin\theta \tag{1.1}$$

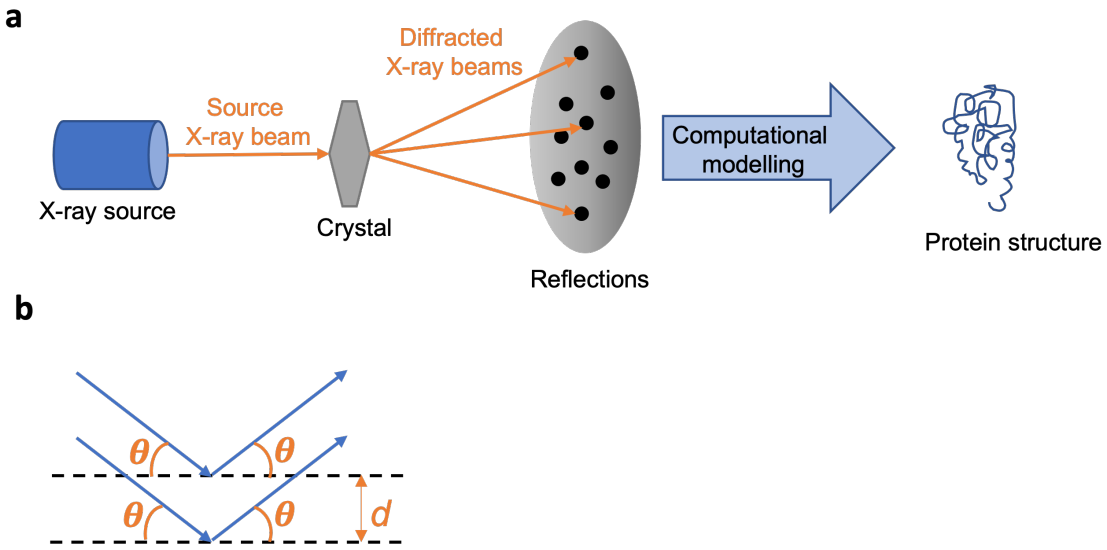

Figure 1.2: (a) An overview of a typical crystallography setup where an X-ray source is used to illuminate a crystal. Diffracted X-rays are then detected as reflections on a detector and the reflections are used with computational modelling to solve the protein structure. (b) A visualization of how constructive interference emerge from two X-rays reflected, at an angle θ, against two parallel crystal planes, separated at a distance d.

After collection of diffraction data, a model of the molecular structures in the asymmetric unit of the unit cell can be determined using advanced algorithms (11). The algorithms are used to calculate the electron-density in the asymmetric unit, to create a so-called electron-density map. The calculations are based on information given by the detected reflection intensities, which carries information of the atomic positions in the unit cells. Each diffracted X-ray beam, and hence each reflection, is characterised by a structure factor (F), which represent the reflection amplitude ($|F|$) and phase (ϕ). However, only the amplitudes can be obtained from the measured reflection intensities, the phases on the other hand needs to be calculated.

The phases can be calculated with different methods. However, the general procedure of the methods is to first calculate an approximate model of the electron-density distribution in the unit cell and thereafter improve the model in an iterative manner (11). One method to obtain initial phases for calculating the electron-density is to use molecular replacement (MR). Known phases of a homologous molecule, or the same molecule crystallized previously, are then used. The approximate model is then refined to improve the agreement between the experimentally observed reflection amplitudes ($|F_{obs}|$) and the amplitudes calculated from the model ($|F_{calc}|$).

The structure of the molecules in the unit cell are determined by interpreting the electron-density distribution, which contains information of which parts of the unit cell that are occupied by atoms

(11). During refinement of the structure model, manual modelling is often used to fit the structure model to the electron-density map. While refining the structure model, a new electron-density map is calculated using Fourier transformation on the observed reflection amplitudes $|F_{obs}|$ and and their phases calculated from the current model ϕ_{calc} (the first refinement uses the phases of the structure model used with MR).

Manual modelling of the structure model utilizes the electron-density map (F_{obs}) together with a so-called difference map (F_{obs}-F_{calc}), where F_{obs} and F_{calc} are the structure factors representing the observed or calculated structure factor amplitudes and the calculated phases. The electron-density map is an approximation of the true structure and the difference map indicates differences between the true structure and the model. The difference map is calculated from the difference between the observed and calculated structure factors and indicates parts of the model that are missing or have wrongly introduced atoms to the model, by showing positive respectively negative contours. Superposition of the two maps, giving a $2F_{obs}$-F_{calc} map, is commonly used together with the difference map during manual modelling. The $2F_{obs}$-F_{calc} map and the F_{obs}-F_{calc} map are typically contoured at 1σ respectively $\pm 3 - 3.5\sigma$, where σ is the standard deviation of the overall electron density from the average electron density.

The quality of the derived structure model is most commonly validated with R-factors (or residuals), root-mean-square deviations (rmsd) from stereochemical standards and Ramachandran plots (11). The R-factors determine deviations between the experimentally measured structure-factor amplitudes, $|F_{obs}|$, and the ones calculated from the model, $|F_{calc}|$, by the following equation:

$$R = \frac{\sum \parallel F_{obs} \mid - \mid F_{calc} \parallel}{\sum \mid F_{obs} \mid} \tag{1.2}$$

A R-factor value of zero indicates a perfect fit between the experimentally measured structure-factor amplitudes and those calculated form the model. However, this is never the case in protein crystallography and a R-factor of around 20% are commonly considered acceptable (11). To avoid over-fitting the model, through including parameters not justified by the experimental data, a small subset of around 5% is most often excluded from the data before model refinement and from which a R_{free} value is calculated. By comparing the R-factors calculated from the data used in refinement, often referred to as R_{work}, with R_{free}, one can identify if the model has been over-fitted. R_{free} will always be larger than R_{work}, but caution should be taken so that the values

doesn't differ too much as it indicates over-fitting (11).

1.1.2 Protein crystallization

The production of well-diffracting protein crystals may be a challenging and time consuming step in crystallography. It's hard to predict under what conditions individual proteins crystallize and there is hence a need for screening different crystallization conditions. These conditions include selection and concentration of precipitant, concentration of protein, temperature and pH (12).

The most common procedure used to form protein crystals is to exert a controlled precipitation of protein in solution, without denaturing it (3). This is done by mixing purified protein with a buffer containing a precipitating agent, or precipitant. There are different types of precipitants, for example salts, organic solvents and high molecular weight polymers (12). The different precipitants acts by different mechanisms, but all acts to reduce the protein solubility to provoke protein-protein interaction and crystal formation.

The event of protein crystallization from influencing the protein and precipitant concentrations can be visualized in a two-dimensional phase diagram, as seen in Figure 1.3(a). To form crystals, the protein concentration must reach supersaturation to enter the nucleation and metastable zones. During nucleation, some protein molecules interact to form nuclei. This in turn lowers the concentration of soluble protein until the metastable zone is entered. In this zone, protein molecules will bind to the nuclei to produce larger crystals until the soluble protein concentration has decreased to an undersaturated level (12). The more nuclei formed in the nucleation zone, the more and the smaller crystals will be produced in the metastable zone. One way of increasing the number of nucleation sites that can be further grown in the metastable zone is to add seeds, which will be further discussed in section 1.1.2.

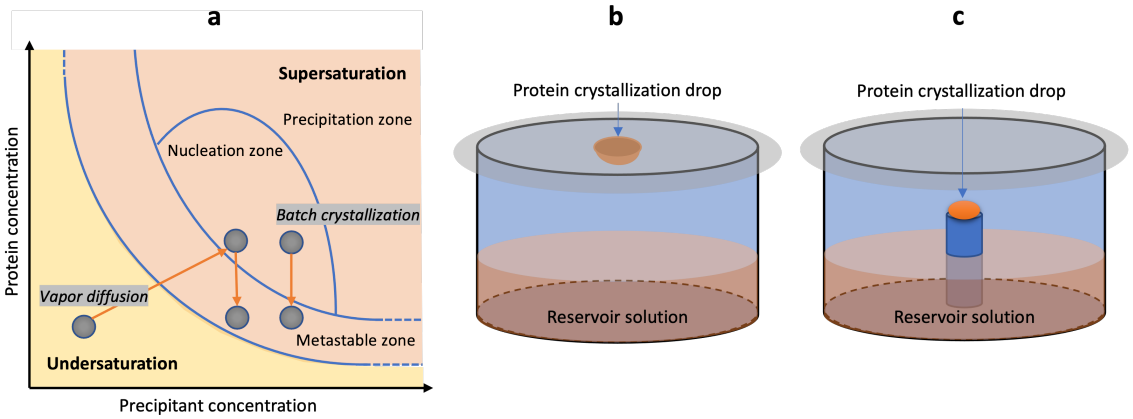

Figure 1.3: (a) A phase diagram showing the different protein crystallization phases entered as a function of protein- and precipitant concentration. The grey circles together with the orange arrows shows the mechanisms under which vapor diffusion and batch crystallization operates. (b,c) Experimental setup for crystallization with the (b) hanging-drop and (c) sitting-drop techniques.

Protein crystallization techniques

Different techniques are used to bring the protein to supersaturation and induce crystallization. The two most common techniques are vapor diffusion and batch crystallization. For experiments using the vapor diffusion technique, a drop composed of protein and precipitant is equilibrated against a reservoir solution of higher precipitant concentration, causing vapor to diffuse from the drop to the reservoir (12). The crystallization is conducted in a closed environment and as vapor diffuses from the drop, the protein and precipitant concentrations slowly increase which brings the protein into supersaturation, Figure 1.3(a). In contrast, for batch crystallization experiments, supersaturation is reached directly when mixing the protein and precipitant solutions, Figure 1.3(a). No vapor diffusion does hence occur for batch crystallization.

Both vapor diffusion and batch crystallization can be used with hanging- and sitting-drop experimental setups, Figure 1.3(b,c). The protein-precipitant drop is then either hanging on a cover slip over the reservoir solution, or sitting on a shelf inside the crystallization container. When using batch crystallization, the reservoir solution has the same precipitant concentration as the drop to eliminate vapor diffusion. In addition to the hanging- and sitting-drop techniques, batch crystallization can be performed by immersing the crystallization drop in an inert oil (microbatch method) or by mixing protein and precipitant in a closed container (12).

Production of microcrystals

By adjusting the crystallization conditions, one can promote formation of either a few large macrocrystals or many small microcrystals. In SX, tens to hundreds of thousand microcrystals are used, ranging in size from submicro- to tens of micrometers. This stresses the need for an efficient way of producing microcrystals. One method that has shown successful is to use seeding (13). Small crystalline fragments are then added to the crystallization drop to increase the number of nucleation sites and bring the drop directly into the metastable zone where crystals can grow. One way of producing seed is to crush large crystals into smaller fragments (13).

Crystallization of protein-ligand complexes

The structural determination of ligands binding to proteins is of significant importance in modern drug design and development, of which a major part is focused on structure-based ligand design (1). In structure-based ligand design, small organic molecules (100-300 Da), referred to as fragments, are utilized. These are often identified through screening experiments with a high sensitivity for detecting weak binders. Structural information of how the fragments binds to the target protein can be used for designing a larger ligand with more drug like properties, such as higher affinity for the protein. This can be achieved by expanding one fragment or merging several fragments. Structure-based design can hence be used to design effective drugs by reserving key-interactions identified between the fragment(s) and the protein.

Based on the two methods for producing crystals of protein-ligand complexes, soaking and co-crystallization, co-crystallization is of particular interest as it doesn't require any modifications to be made on the crystals. The principle of co-crystallization is to allow the protein to bind the ligand prior to forming crystals. As previously mentioned, co-crystallization can be performed by incubating ligand and protein in solution prior to setting up crystallization drops (1) or to pre-coat fixed-target supports with ligand before adding a protein crystallization solution, referred to as solution- and dry-co-crystallization. The latter technique has previously been used to study macro-crystals grown on ligand-coated 96-well plates compatible with *in situ* diffraction (10). Drops of ligand diluted in dimethyl sulfoxide (DMSO) was then added to the plate, followed by solvent evaporation for a week in room-temperature. By performing co-crystallization directly on fixed-target supports allows for a complete elimination of required crystal handling steps, which wouldn't be possible with soaking experiments.

1.1.3 Room-temperature serial synchrotron crystallography

SX has been successfully implemented at both XFELs and synchrotrons (8). SX at XFELs is performed by exposing the crystals with X-ray pulses of high intensity and very short exposure times (femtoseconds). The short exposure time allows for collection of data in RT before the crystals are destroyed by radiation damage, which is a phenomena caused by diffusion of free radicals in the crystal which constitutes an issue for conventional crystallography (4). Synchrotrons doesn't have as short exposure time as XFELs but through several improvements of the synchrotron facilities, for example shortening the sample exposure time, radiation damage can be avoided also for SSX (8). Globally, there are much more synchrotron facilities than XFELs, resulting in a greater beam time availability at synchrotrons. Due to this, there has been an increased interest of performing SX at synchrotrons, which also has been leading to the construction of beamlines specifically dedicated for SX (8; 14).

Synchrotrons are large facilities that accelerates electrons in a storage ring (15). The electrons are produced and accelerated in a linear accelerator (LINAC) prior to being injected to the storage ring. The storage ring is equipped with a set of magnets used to change the direction of straight moving electrons. As the path of the electrons is changed, energy is released as X-rays. The emitted X-rays are directed towards experiment hutches (beamlines) where the crystallography experiments are performed. The synchrotron at the MAX IV Laboratory, at which the experiments in this project were performed, was the first synchrotron with a 4th generation storage rings in operation worldwide (8; 15). In this project, the RT-SSX experiments were performed at the BioMAX beamline which is connected to the 3 GeV storage ring of the synchrotron, Figure 1.4 (16).

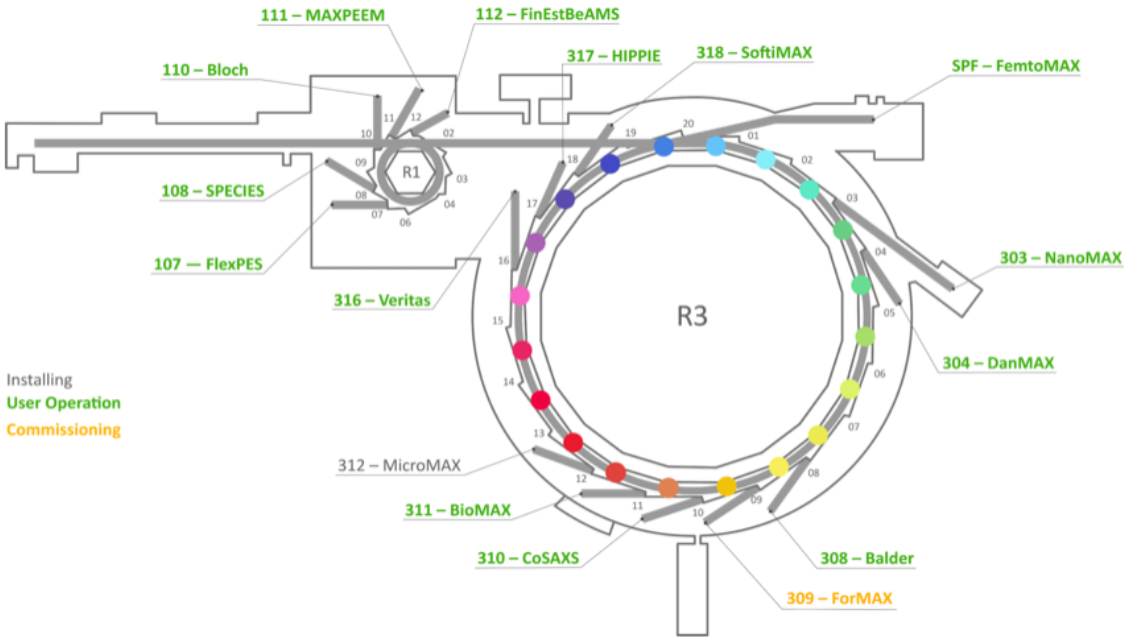

Figure 1.4: Schematic representation of the storage rings (R1 and R3) and beamlines at the MAX IV Laboratory. Source: Adapted from (16).

Sample delivery techniques for SSX

The microcrystals used for SSX can be introduced to the X-ray beam with injection or fixed-target techniques. One of the injection techniques available at synchrotrons is the high-viscosity extrusion (HVE) injector and there are several different fixed-target supports available. The fixed-target sample delivery method have in some cases shown superior as it can provide a much lower sample consumption compared to injection with HVE (8). The different fixed-target supports may vary regarding for example tolerance for room- or cryogenic temperatures, prevention of crystal dehydration, data collection rate and the amount of X-ray background generated (7). When it comes to X-ray background, supports made of polyimide or silicon nitride have shown profitable as they generate little background (7). Another difference between supports may be whether it's possible to perform crystallization directly on the supports or not. Being able to perform on-chip crystallization is of particular interest for fragile crystals as it lowers manual handling steps of these.

Several fixed-target supports of different designs have been successfully used for RT-SSX. Depending on the support design, different experimental setups are required at the synchrotron. Supports for which the protein drop(s) (8) or naked protein crystals (17) are exposed to air, a humidifier is needed to keep the crystals hydrated. On the other hand, the need of a humidifier

can be avoided in cases where the drop can be sandwiched between two supports (9; 8).

At MAX IV, two different types of fixed-target supports are used, these are silicon nitride membranes (Silson, UK) and XtalTool (Jena Bioscience, Germany) made of bio-inert polyimide (8). Sandwiches can be produced with the membranes to keep the crystals hydrated for at least 30 minutes, whereas a humidifier is needed for the XtalTools as these can't be sandwiched. When it comes to on-chip crystallization on the supports, it has been successfully used with the XtalTools. However, off-chip crystallization followed by loading the crystals on the support is most commonly used with the membranes (8). It is therefore of interest to evaluate the opportunity to perform on-chip crystallization on these membranes to lower the crystal handling steps.

1.2 Aim

The overall aim of the project was to investigate the possibilities of using on-chip co-crystallization on standard silicon nitride membranes (Silson, UK) with RT-SSX, in order to reduce the crystal handling steps and to envision the opportunities of using the method in drug design and development research. To achieve this, the aim was divided into two parts:

- Firstly, to investigate the potential of growing crystals suitable for RT-SSX using on-chip crystallization of the proof-of-concept protein sEH on the silicon nitride membranes.
- Secondly, to evaluate the possibilities of producing ligand complex structures of sEH using on-chip co-crystallization on the silicon nitride membranes, with the dry- and solution-co-crystallization techniques. The capability of the two co-crystallization techniques were evaluated with RT-SSX at BioMAX.

2. Materials and metods

2.1 Protein crystallization drop constituents and materials

2.1.1 Protein

The protein used in the project was produced at the department in 2020 and had since then been stored at -80℃. sEH was then produced in *Spodoptera frugiperda* Sf9 cells and purified using nickel-affinity and size-exclusion chromatography. Purified protein of 16 mg/mL was contained in a buffer of 20 mM Tris hydrochloride (HCl) pH 8, 150 mM NaCl, 1 mM TCEP and 10% glycerol.

2.1.2 Ligands

Three ligands obtained from AstraZeneca were used for co-crystallization with sEH. The ligands were 2-(1H-benzimidazol-2-ylsulfanyl)ethanol (6N4), 5-cyclohexyl-1,3-dihydroindol-2-one (FCW) and 6-bromo-1,3-dihydro-2H-indol-2-one (1P8), of molecular weights 194.3, 215.3 and 212.1 Da respectively. All ligands were provided in 500 mM stock solutions diluted in DMSO. Furthermore, a cryo-structure of the sEH-ligand complexes was available for all ligands and reported in PDB as 5akj (sEH-6N4 complex structure), 5ald (sEH-FCW complex structure) and 5akk (sEH-1P8 complex structure)

2.1.3 Precipitants

The precipitant solution used in the protein crystallization drops was prepared from stock solutions purchased from Hampton Research. The solutions were 50% w/v Polyethylene glycol (PEG) 3,350 Monodisperse (CAT NO. HR2-527), 2.0 M Lithium sulfate monohydrate ($Li_2SO_4 \bullet H_2O$) (CAT NO. HR2-545) and StockOptions Tris HCL 16 (1.0 M Tris hydrochloride pH 8.5, CAT NO. HR2-937-16).

2.1.4 Seed

Seed was used to increase the number of nucleation sites in the crystallization drops and was produced by crushing macro-crystals, grown by vapor diffusion as described in Appendix A. The crystals were transferred from crystallization plates to a 2 mL Eppendorf tube and vortexed with two MicroSeed Beads (Molecular Dimensions, CAT NO. MD2-14) for approximately 20 minutes. The solution was sporadically cooled on ice to avoid crystal melting. The seed solution was judged under a light microscope and approved as no large crystal fragments could be seen.

2.1.5 Crystallization plates and fixed-target supports

The 24-well crystallization plate Cryschem M Plate (round reagent reservoir) (Hampton Research, CAT NO. HR1-002) was used for screening optimal sEH-crystallization and co-crystallization conditions, using the sitting-drop technique. The plate was additionally used to create sealed containers for growing crystals on the fixed-target supports standard silicon nitride membrane (SiRN-5.0-200-2.5-1000, Silson, UK). The membranes used had a size of 2.5 mm x 2.5 mm and a thickness of 1000 nm, and were placed on the drop shelves of the Cryschem M crystallization plates. The crystallization plates were sealed with ClearSeal Film (Hampton Research, CAT NO. HR4-521) to avoid drop evaporation and maintain stable batch-crystallization conditions.

2.2 Screening of protein crystallization conditions

2.2.1 Production of sEH microcrystals

Microcrystals of sEH were grown using sitting-drop batch crystallization, according to a protocol previously developed at the department. Crystallization drops of protein and seed-containing precipitant solution were set up with a reservoir solution of protein buffer and precipitant solution, where the precipitant solution was composed of 34% w/v PEG 3,350, 0.1 M $Li_2SO_4 \bullet H_2O$ and 0.1 M Tris HCl pH 8.5. Furthermore, 10% v/v diluted seed stock-solution was added to the precipitant solution, prepared as described in the following paragraph.

To increase the number of well-sized microcrystals (10-20 µm in width) in the crystallization drops, screening was performed where different protein-precipitant ratios and different dilutions of the seed stock-solution were evaluated. The protein-precipitant ratios investigated were 1:1, 1:2, 1:3, 1:4, 1:5 and 1:6 (i.e. one part protein together with one to six parts of precipitant solution). The seed stock-solution, produced as described in section 2.1.4, was diluted in ratios of 1:48,

1:64 and 1:128 with 40% w/v PEG 3,350, 0.1 M $Li_2SO_4 \bullet H_2O$ and 0.1 M Tris HCl pH 8.5. The diluted seed solutions were then further diluted in a 1:9 ratio with 34% w/v PEG 3,350, 0.1 M $Li_2SO_4 \bullet H_2O$ and 0.1 M Tris HCl pH 8.5, prior to being added to the drop precipitant solution.

The initial screening experiments were performed in the crystallization plates using 2-7 µL crystallization drops, grown using sitting drop crystallization. While going over to crystallization on the silicon nitride membranes, the sitting drop posts of the crystallization plates were used to hold the membrane in a horizontal position. All on-chip crystallization experiments on the membranes were performed with 2 µL drops, as that's the maximum volume that two sandwiched membranes could accommodate. All crystallization experiments were further set up with a 500 µL reservoir solution, where the ratio of protein-buffer and precipitant solution was the same the protein-precipitant ratio of the drops (ie. 1:1-1:6). When the crystallization plates were fully prepared with drops and reservoir solution, ClearSeal Film was used to cover it.

2.2.2 Co-crystallization

The possibilities to obtain microcrystals of sEH co-crystallized with the three ligands 6N4, FCW and 1P8 was investigated with the two techniques dry- and solution-co-crystallization.

Dry-co-crystallization

Using the dry-co-crystallization technique, the ligands were dried on the concave sitting-drop posts on the crystallization plates or on the silicon nitride membranes prior to setting up crystallization drops. The ligands were diluted to 5-50 mM in DMSO and thereafter dried on the crystallization plates or membranes for 24h in a 37℃ incubator. A drop volume of 1 µL was shown to be enough to cover the whole membrane surface, and was therefore used for all experiments. When the ligand drops had dried, protein-precipitant drop solutions, prepared in accordance with the description in section 2.2.1, were mixed and immediately added on the ligands.

Solution-co-crystallization

Using the solution-co-crystallization technique, ligand in solution was mixed with the protein-precipitant crystallization drops. In the first experimental setups, the ligands were diluted in the precipitant solution, to concentrations of 1-15 mM. However, to increase the chances for the protein to bind the ligand prior to crystallizing, the ligand was diluted with the protein in a second experiment, to concentrations of 5-20 mM. The protein-ligand solution was then

incubated in room temperature for up to 6h prior to setting up crystallization drops. For both experiments, the crystallization drops were set up according to the description in section 2.2.1.

2.2.3 On-chip crystallization

To investigate the best procedure to perform on-chip crystallization on the silicon nitride membranes, two different methods were evaluated. The first method evaluated was to grow the crystals sandwiched between two silicon nitride membranes, whereas the second method was to grow the crystals on one membrane, exposing the upper surface of the drop to the air. The performance of the two methods was evaluated against control drops grown on the sitting drop posts of the crystallization plates.

2.3 RT-SSX at BioMAX

During the project, two beamtimes were attended at the BioMAX beamline at the MAX IV Laboratory. However, successful data collection was only obtained from the second beamtime. At the first beamtime, the samples analyzed were prepared and shipped from Gothenburg to Lund. However, the crystals didn't diffract well, which was believed to be caused by crystal dehydration during the transportation. Therefore, the crystals analyzed at the second beamtime were grown on-site at MAX IV the day before the experiment. The following sections hence refers to the samples prepared and analyzed at the second beamtime. Furthermore, the crystallization conditions and the ligand used to produce the on-chip co-crystallized samples were selected based on the most promising results from the screening experiments.

2.3.1 Samples

Samples of sEH co-crystallized with 6N4 was grown on the silicon nitride membranes for 18-24h prior to RT-SSX analysis. Three samples prepared with the dry-co-crystallization technique were analyzed, where 1 µL 20 mM ligand diluted in DMSO was dried on the membranes. Furthermore, five samples prepared with the solution-co-crystallization technique were analyzed, where protein was incubated with 5 mM ligand for 3h. The crystallization drops were set up in a 1:2 protein-precipitant ratio and with a seed-dilution of 1:48. For all samples, a second membrane was added on top of the crystal drops, creating a sandwich, just before the X-ray analysis. The sandwiches were aligned in front of the X-ray beam by being mounted to a goniometer, Figure B.1 in Appendix B.

2.3.2 Data collection and processing

All data was collected at BioMAX, with a detector distance that corresponds to a resolution edge of 1.80 Å on the detector, a beam size of 20 µm × 20 µm, a photon flux of about $1{\times}10^{12}$ photons s^{-1} and with an exposure time of 0.01 s per collected image.

Initial data processing including initial hit identification, indexing, scaling and merging of the data was performed using software within the CrystFEL version 0.9.1 suite, whereof indexing, merging and integration was performed using the crystal unit cell $P6_522$, as it has previously been observed for RT-sEH structures (Dunge *et al.*, in preparation) as well as for the sEH-6N4 cryostructure (PDB code 5akj) (1). Software within the Collaborative Computational Project Number 4 (CCP4) suite were thereafter used to truncate and phase the data followed by refining the structure models. The data was truncated using TRUNCATE and phased by molecular replacement (MR) with Phaser, using a water-free apo-sEH cryo-structure, solved at the department (Dunge *et al.*, in preparation), as a search model. The structure models were then manually modelled using COOT and refined using REFMAC5, where around 5% of the data was excluded from the refinement to avoid over-fitting.

Finally, the two RT-structures solved from the sEH-6N4 co-crystallized samples were compared with the sEH-6N4 cryo-structure 5akj.

3. Results

3.1 Characteristics of crystals grown under different conditions

3.1.1 The effect of drop ratio and seed dilution on the number and size of crystals

By varying the drop ratio of the crystallization drops it was found that drops of protein-precipitant ratio 1:1 gave the most uniform crystals but also generated a high amount of precipitate, Figure 3.1(a,b,c). On the other hand, drops of ratio 1:2-1:6 didn't present any precipitation but the crystals were less uniform, Figure C.1 in Appendix C. Furthermore, it could be seen that while increasing the fraction of seed-containing precipitant solution in the drops, from 1:1 to 1:6, the size of the crystals tended to decrease, Figure C.1 in Appendix C.

The effect of varying the dilution of the seed, using the three dilutions 1:48, 1:64 and 1:128, clearly showed that a high dilution generated fewer but larger crystals and a low dilution generated more but smaller crystals, when comparing drops having the same drop ratio, Figure 3.1(a,b,c). By analyzing drops having different drop ratios and seed dilutions, the best condition was identified for drops of ratio 1:2 and seed dilution of 1:48, Figure 3.1(d). These conditions were hence used for producing the samples analyzed at BioMAX.

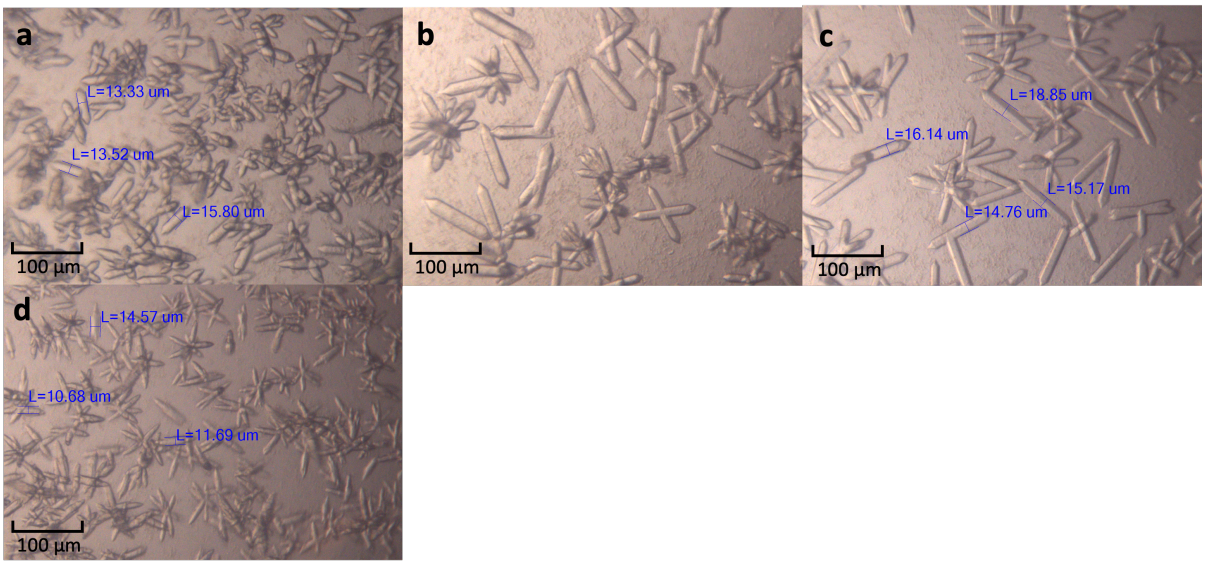

Figure 3.1: Screening of the effect of varying the protein-precipitate ratio of the crystallization drops and the seed concentration. The crystals were grown on the Cryschem M crystallization plates. (a,b,c) Crystals grown in drops with a protein-precipitate ratio of 1:1 and a seed dilution of (a) 1:48, (b) 1:64 and (c) 1:128. (d) Crystals grown in a drop of seed dilution 1:48 and protein-precipitate ratios of 1:2.

3.1.2 The capability of different ligands to be used for co-crystallization with sEH

Co-crystallization of sEH with the three ligands 6N4, 1P8 and FCW presented crystals of varying sizes together with different amount of precipitate. Using both the dry- and solution-co-crystallization techniques, co-crystallization with 1P8 showed the least profitable crystal characteristics for being analyzed by SSX. Using the dry-co-crystallization technique, by drying 1µL 5 mM ligand diluted in DMSO on silicon nitride membranes, ligand 1P8 generated smaller crystals and significantly more precipitate compared to the other two ligands, Figure 3.2(a,b,c). Furthermore, using the solution-co-crystallization technique, by diluting the ligands to 3.4 mM in the precipitant solution, two distinct crystal populations were found in drops with 1P8. However, a second crystal population was not observed for co-crystals with either 6N4 or FCW, Figure 3.2(d,e,f).

Co-crystallization with 6N4 and FCW, using the two different techniques, showed almost as good characteristics. However, crystals grown using the solution-co-crystallization technique, generated slightly thicker crystals for 6N4 compared to FCW, 3.2(d,e), leading to the selection of 6N4 for the SSX experiments at BioMAX. Optimization of the two co-crystallization techniques were hence mainly focused on co-crystallization with 6N4.

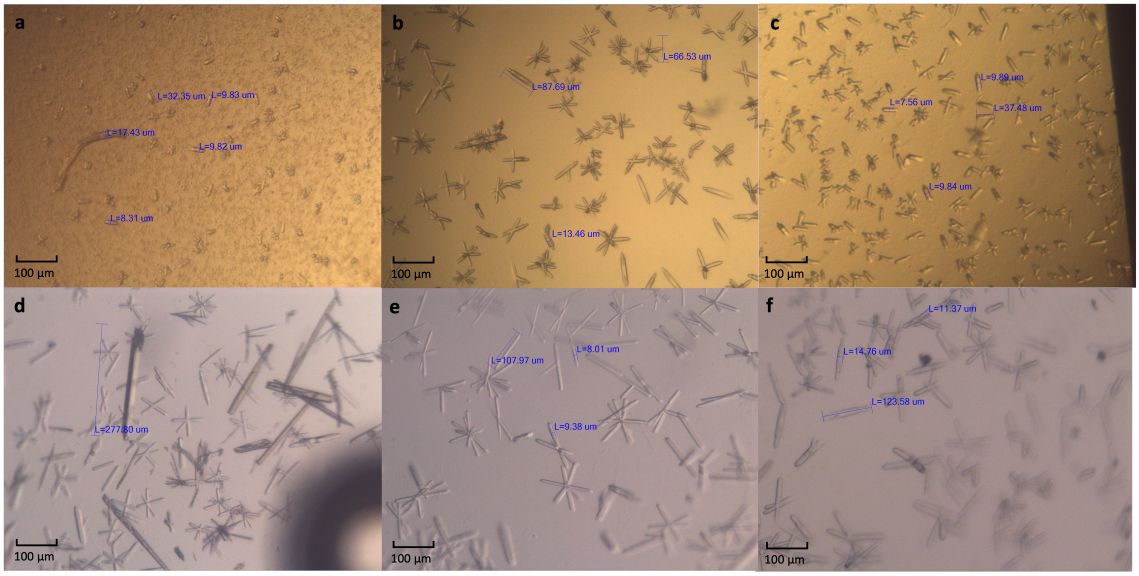

Figure 3.2: Co-crystallization of sEH with (a,d) 1P8, (b,e) FCW and (c,f) 6N4, using the (a,b,c) dry-co-crystallization technique and the (d,e,f) solution-co-crystallization technique. The dry-co-crystallization experiments were performed on silicon nitride membranes by drying 1µL 5 mM ligand diluted in DMSO on the membranes, leading to a final ligand drop concentration of 2.5 mM if all ligand would dissolve. Co-crystallization with (a) 1P8 and (b) FCW were performed under the same conditions, whereas drops with (c) 6N4 used a higher seed dilution which can explain the difference in crystal number and sizes. The solution-co-crystallization drops were grown on the Cryschem M crystallization plates. The ligands were diluted in the precipitant solution to a concentration of 3.4 mM. Length and width measurements of some selected crystals are shown in the images.

Development of the dry-co-crystallization technique

The dry-co-crystallization technique was initially performed on the Cryschem M crystallization plates by drying the ligands diluted in DMSO, on the concave drop shelves of the plates. After adding the crystallization drops, it was found that the dried ligands resolved poorly in the drops, Figure 3.3(a,b). There was hence a concern that unresolved ligand would generate unwanted background in an SSX analysis. However, as moving on to dry the ligands on the flat silicon nitride membranes, the ligands ended up predominantly at the membrane edges, leading to less debris among the crystals and hence a lower risk of background, Figure 3.3(c,d).

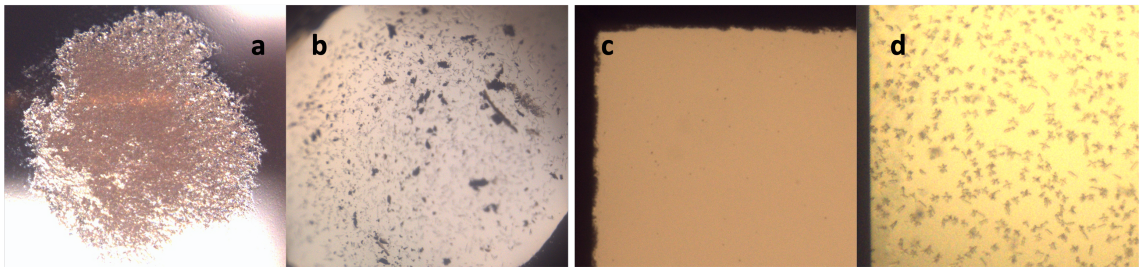

Figure 3.3: Ligand 6N4 dried on (a) Cryschem M crystallization plates and (c) silicon nitride membranes. (c) The dried ligand ended up predominantly at the membrane edges (between the light brown membrane and the black membrane frame). Crystals grown in drops added on top of the dried ligand in (b) Cryschem M crystallization plates and (d) silicon nitride membranes.

Development of the solution-co-crystallization technique

The first experiments using the solution-co-crystallization technique was performed by diluting the ligand in the precipitant solution. However, several crystallization experiments during the project showed that the size of the sEH crystals changed very little after being grown for around 2h, 3.4(a,b). As it was shown that the protein crystallized fast, incubation of protein and ligand was evaluated to increase the chances of forming protein-ligand complexes prior to crystallization. By diluting ligand 6N4 to 5-20 mM in protein, some precipitate was identified in the drops. However, by incubating the solutions for 3 and 6h, the amount of precipitate in the drops were reduced, Figure 3.4(c,d,e).

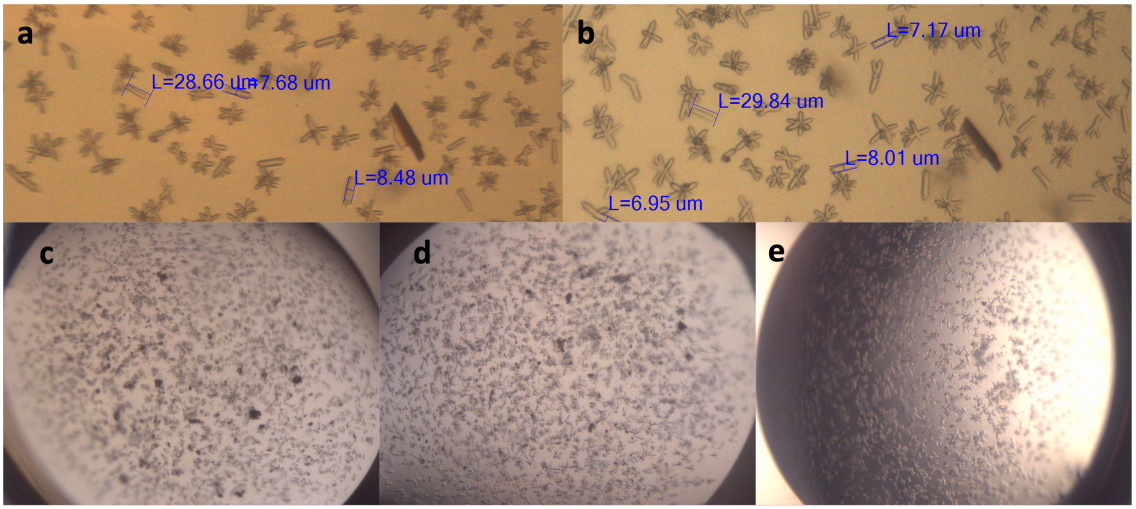

Figure 3.4: (a,b) Comparison of the crystals sizes after being cultured on silicon nitride membranes for (a) 2h respectively (b) three days. (c,d,e) Crystal drops of sEH co-crystallized with 6N4, set up after protein-ligand incubation for (c) 0h, (d) 3h and (e) 6h.

3.1.3 On-chip crystallization

Crystals grown on silicon nitride membranes generated crystals of a similar shape and in a similar amount as crystals grown on Cryschem M crystallization plates. However, the crystals differed significantly in size depending on if the drops were exposed to the surrounding air or enclosed between two membranes in a sandwich. The first crystallization setup evaluated was to crystallize the protein between two membranes, as this would facilitate transportation of the samples. However, the crystals grown in sandwiches were thinner (around 5 µm in width), compared to crystals grown in control drops on the crystallization plates (around 10-15 µm in width), Figure 3.5(a,b). Therefore, crystallization on the membranes was evaluated by growing crystals without a second membrane added on top of the drops. Overall, the crystals grown in drops exposed to air were slightly bigger (up to around 14 µm in width) compared to crystals grown sandwiched between two membranes (generally smaller than 10 µm in width), Figure 3.5(c,d).

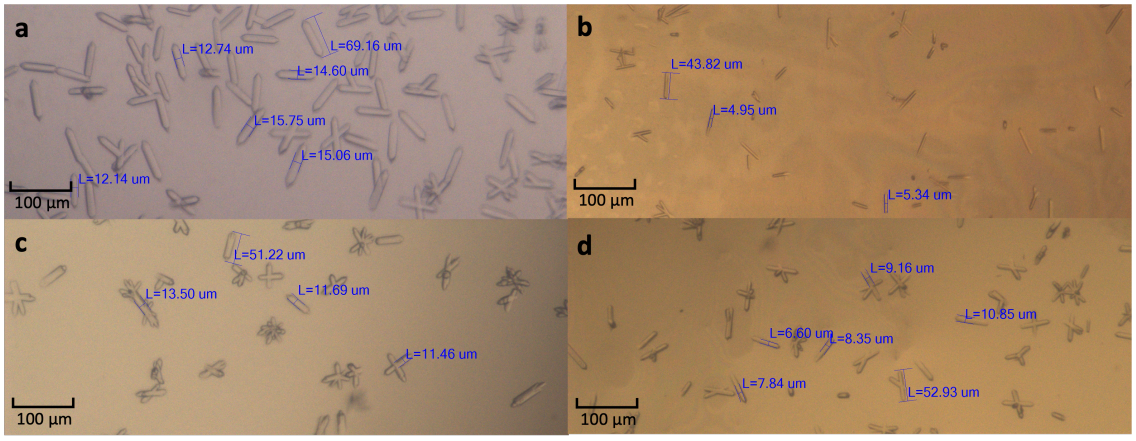

Figure 3.5: (a,c) Crystals grow in drops exposed to air or (b,d) enclosed between two silicon nitride membranes in a sandwich. (a) The crystals grown on the Cryschem M crystallization plates were used as controls for (b) the crystals grown between two sandwiched silicon nitride membranes, showing that the crystals grown between the sandwiched membranes were thinner than the controls. Similarly, the sizes of crystals grown (d) in sandwiches were thinner than crystals grown (c) on only one the membrane with the drop upper surface exposed to the air. Length and width measurements of selected crystals are shown in the images.

3.2 RT-structures of the sEH-6N4 complex solved from the dry- and solution-co-crystallization samples

Both structures solved from the data collected at BioMAX, for the dry- and solution-co-crystallization samples, clearly showed that the protein bound the ligand. However, the structure

models presented in this report are only preliminary models, and a result of initial refinements. Further modelling and refinements are needed to improve the quality of the structure models.

The resolution of the two RT-structures were of 2.25 and 2.34 Å, for the dry- and solution-co-crystallization samples, respectively. Furthermore, the refined structure models had R_{work} and R_{free} values of 20.26% and 25.21% for the dry-co-crystallization samples and 20.21% and 26.91% for the solution-co-crystallization samples. The large difference between R_{work} and R_{free} for the models indicates the need of further refinements of the structure models. All data collection and refinement statistics for the two RT-SSX solved structures is presented are Table 3.1, together with statistics from the determination of the cryo-structure, 5akj, of the sEH-6N4 complex (1). Regarding the presented statistics of the cryo-structure, several variables could not be found, leading to the high amount of N/A.

3.2.1 Differences between the structures of the dry- and solution-co-crystallization samples

During the first rounds of refining the structure models of the dry- and solution-co-crystallization samples, both structures indicated that the protein potentially bound the ligand. However, the indication was slightly clearer for the structure model of the dry-co-crystallization samples. For this model, the F_{obs}-F_{calc} map showed a larger positive contour volume at the ligand binding site compared to the solution-co-crystallization structure, Figure 3.6. However, after including the ligand in the structure model, followed by further modelling and refinements, it was shown that the ligand fitted the electron density equally well for both structure models. Due to the need for prior approval of AstraZeneca before displaying ligands, the structure models where the ligand is included in the models can't be published in this report.

Table 3.1: Data collection and processing statistics.

Parameter	**RT-SSX, dry-co-crystallization**	**RT-SSX, solution-co-crystallization**	**Cryo-crystallography, soaking**
PDB code	N/A	N/A	5akj
Total amount of sample used (µL)	6	10	N/A
Data collection			
Average flux dimension (ph/s)	1.3×10^{12}	1.1×10^{12}	N/A
Beam size (µm × µm)	20 × 20	20 × 20	N/A
Data collection temperature (K)	293	293	100
Exposure time per image (s)	0.01	0.01	N/A
No. of collected images	48 953	83 467	N/A
No. of hits	16 881	30 685	N/A
Average hit rate (%)	34.5	36.7	N/A
No. of indexed images	13 887	27 083	N/A
Indexing rate (%)	28.4	32.4	N/A
No. of total / unique reflections	7 221 473 / 151 704	56 794 860 / 263 261	N/A / 40 145
Multiplicity	47.60	215.74	N/A
Space group	$P6_522$	$P6_522$	$P6_522$
Cell dimensions *a, b, c* (Å)	94.25, 94.25, 247.58	94.29, 94.29, 247.61	92.57, 92.57, 244.22
Cell dimensions α, β, γ (°)	90, 90, 120	90, 90, 120	90, 90, 120
Completeness (%)	100	100	98.5 (97.5)
$I/\sigma(I)$†	2.39 (0.55)	5.91 (0.46)	19 (2.6)
Resolution range (Å)†	68.14-2.25 (2.29-2.25)	81.66-2.34 (2.36-2.34)	244.22-2.03 (2.14-2.03)
R_{split}†	24.43 (123.37)	18.09 (16.46)	N/A
CC*†	91.34 (32.99)	94.87 (31.69)	N/A
Refinement			
$R_{\text{work}}/R_{\text{free}}$	20.26/25.21	20.21/26.91	18.4/22.3
No. of atoms (molecules‡)			
Total	4574	4511	4886
Protein	4457 (546)	4434 (546)	4359 (546)
Water	94 (94)	44 (44)	484 (484)
Ligand 6N4	13 (1)	13 (1)	13 (1)
DMSO	0	0	20 (5)
SO4	10 (2)	20 (4)	10 (2)
Rmsd bond length (Å)	0.0083	0.0077	0.010
Rmsd bond angle (°)	1.6150	1.5877	1.18
Average B value (Å^2)	51.715	46.356	29.12
Ramachandran plot statistics			
Favoured (%)	506 (94.23%)	487 (91.71%)	535 (97.63%)
Outliers (%)	6 (1.12%)	6 (1.13%)	1 (0.18%)

† Values in parenthesis are those of the highest resolution shell.
‡ When it comes to the protein, the number of molecules refers to the number of residues.

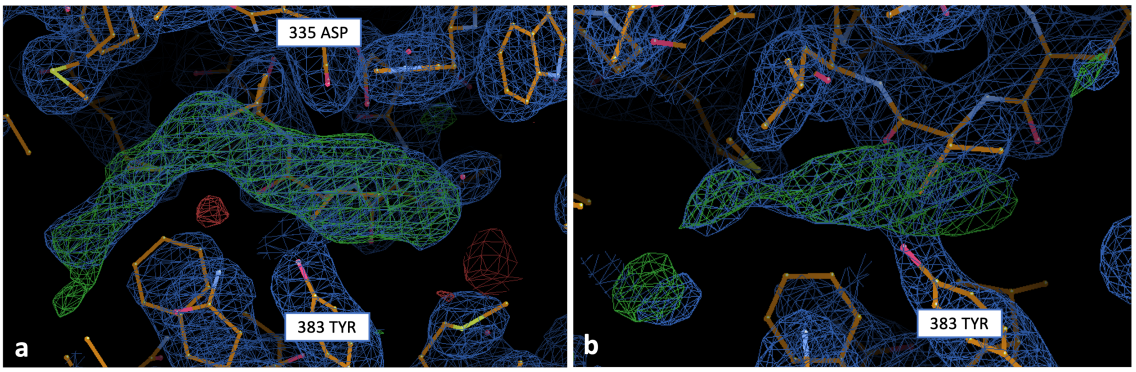

Figure 3.6: Electron-density maps showing the electron-density at the ligand binding site of sEH, for the (a) dry-co-crystallized and (b) solution-co-crystallized samples. The $2F_{obs}$-F_{calc} map is contoured at 1σ and the F_{obs}-F_{calc} map at $\pm 3.5\sigma$. The two protein residues 335 ASP and 383 TYR are marked to give reference points to localize the position in the models.

3.2.2 Comparison of RT- and cryo-structures of the sEH-6N4 complex

Overall, the RT- and cryo-structure of the sEH-6N4 complex, agreed well with each other. Furthermore, the ligand was bound in the same position at both RT and cryogenic temperature. However, some differences between the structures was observed regarding the cell dimensions, water content and position of some protein residues.

Firstly, both RT-structures were about 1.5-3.5 Å larger in each dimension of the unit cell compared to the cryo-structure. Secondly, the water content of the RT-structures were about one fifth, or less, of that of the cryo-structure. Thirdly, differences between the position of some protein residues was predominantly observed for larger protein residues in the exterior parts of the protein. However, a difference was also observed for the phenylalanine residue at position 497 (Phe497), located close to the ligand binding site. Among the residues in the exterior parts of the protein, several residues that were modelled in the cryo-structure had no electron density in the RT-structures. When it comes to residue Phe497, the side-chain was pointing toward the ligand in the RT-structure from the dry-co-crystallization samples, whereas it was pointing away from the ligand in the cryo-structure, 3.7. By analyzing the electron density of both models, it was confirmed that the observed difference was correct. However, for the RT-structure of the solution-co-crystallization samples, residue Phe497 was pointing in the same direction as in the cryo-structure, Figure D.1 in Appendix D.

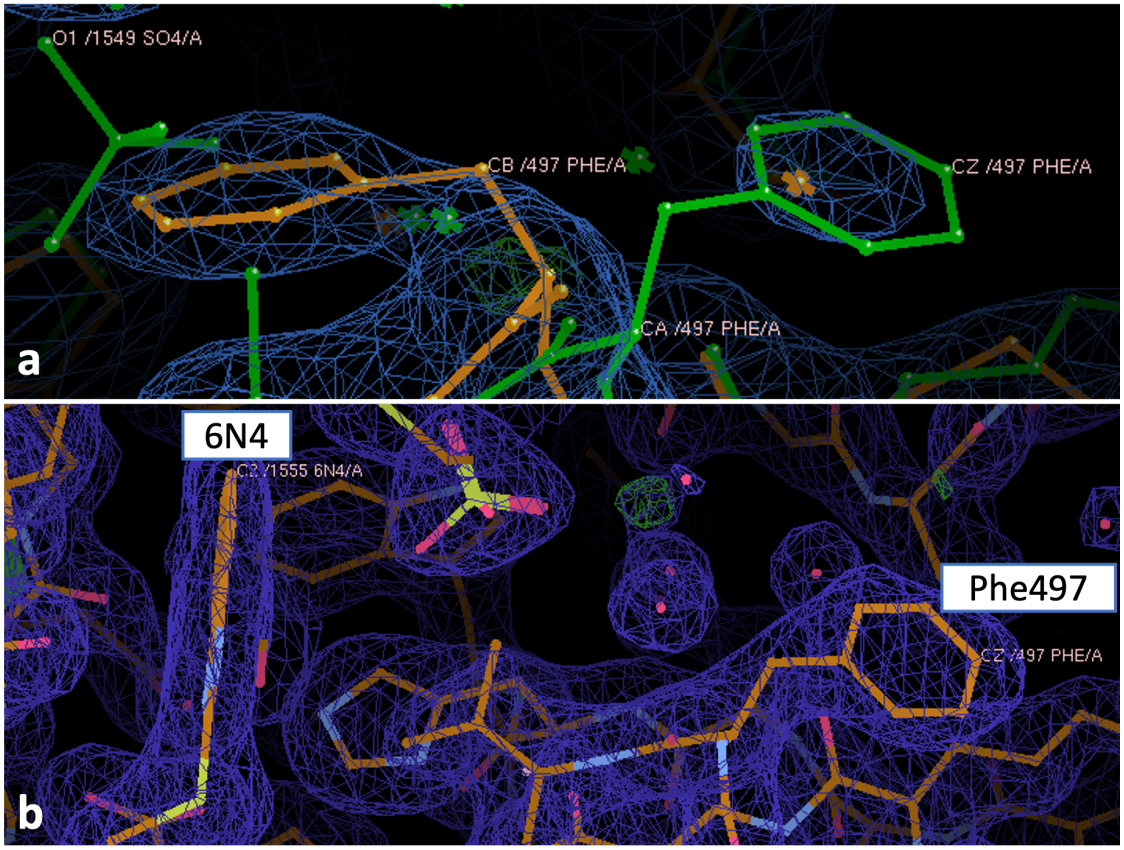

Figure 3.7: Direction of the protein residue Phe497 in the (a) RT-structure form the dry-co-crystallization samples and (b) the cryo-structure of the sEH-6N4 complex. (a) The electron density (blue grid) of the dry-co-crystallization RT-structure (orange), pointing toward the ligand, and the cryo-structure 5akj (green), pointing away from the ligand. (b) The electron density (purple grid) and the cryo-structure 5akj (orange/blue/pink chain). The ligand 6N4 is located to the left of the figures and the Phe497 residue to the right.

4. Discussion

On-chip co-crystallization on the silicon nitride membranes was shown not only to be possible, but also to be capable of producing well-diffracting crystals for RT-SSX using the proof-of-concept protein sEH and ligand 6N4. When on-chip crystallization on the membranes was developed during the project, one of the main obstacles encountered was to obtain a high amount of crystals of sufficient size for RT-SSX. This obstacle is more easily overcome using off-chip crystallization, as crystals then can be spun down in a tube to increase the concentration of crystals loaded on the membranes (18). However, through screening of different crystallization conditions, a condition generating a sufficient amount of well-sized crystals was obtained when crystallizing sEH on the membranes.

Both the dry- and solution-co-crystallization techniques used in this project successfully generated ligand bound protein complexes of sEH and 6N4. However, when it comes to using on-chip co-crystallization in the drug industry, the dry-co-crystallization technique is of particular interest. One reason for the greater interest of this technique is the potential of automating parts of the crystallization procedure (10). Multiple membranes pre-coated with different ligands could be used to screen ligand interactions to a specific target protein. One and the same protein crystallization drop solution could then be added to all membranes, which would facilitate the development of an automated procedure for this step.

Another reason why the dry-co-crystallization technique is of particular interest is the potential of using ligands diluted in DMSO. DMSO is the most commonly used solvent for ligands (1) and the results of this project, together with results from a previous study growing macrocrystals on 96-well plates compatible with *in situ* data collection (10), showed that it's possible to use ligands diluted in DMSO with the dry-co-crystallization technique. This allows for the use of most of the ligands found in chemical libraries. Furthermore, in the study where macrocrystals were grown with the dry-co-crystallization technique, no DMSO molecules were detected on the protein surface, in contrast to cooled crystals soaked with ligands diluted in DMSO. The dry-co-crystallization technique could hence potentially be a good method for producing protein-ligand

bound crystals even for protein crystals sensitive to DMSO, thanks to the absence of DMSO after drying the ligand (10).

Even though on-chip co-crystallization on silicon nitride membranes proved to work in this project, more studies are needed to evaluate the capability of using the method in the drug industry. For example, there is a need for investigating on-chip crystallization of proteins generating crystals of various space groups. In the previous study where the dry-co-crystallization technique was used to produce macrocrystals on 96-well plates, it was shown that space group can affect the number of crystals required for collecting a complete data set (10). The study showed that a full data set could be collected from only one macrocrystal for crystals of the high-symmetry tetragonal space groups $P4_12_12$ and $P4_32_12$, whereas more than one crystal was needed for crystals of the low-symmetry monoclinic space group $P2_1$. In this project, sEH microcrystals of the hexagonal space group $P6_522$ were investigated with *in situ* data collection on the silicon nitride membranes. As *in situ* data collection of macrocrystals required different data collection conditions depending on crystal space group, it's of interest to also investigate the impact of space group for *in situ* data collection of microcrystals used with SSX. Further investigations of on-chip crystallization on the silicon nitride membranes are hence needed to evaluate the capability of using the method with different types of proteins.

Further studies using different types of ligands with on-chip dry-co-crystallization are also needed to evaluate the capability of the method. One ligand characteristic that potentially can affect the use of the technique is solubility. In the previously mentioned study where macrocrystals were grown with the dry-co-crystallization technique, it was found that protein-ligand binding wasn't be observed with some ligands, whereas it was observed when the same ligands were introduced with soaking (10). The reason why no binding was observed with the dry-co-crystallization technique was thought to be due to low solubility of these ligands and weak interactions to the protein. It's hence of relevance to investigate what types of ligands that can be used with the dry-co-crystallization technique also for growing microcrystals for SSX.

To investigate the capability of using the dry-co-crystallization technique it would further be of interest to study proteins which crystallizes at different rates. sEH crystallizes fast compared to many other proteins and it would be interesting to investigate if the crystallization rate affects the possibilities for the protein to bind the ligand prior to crystallization, or if the protein crystallizes prior to binding the ligand. If protein crystallization occur prior to binding the ligand, the ligand could potentially bind in to the crystals. This mechanism would hence be more similar to soaking

than co-crystallization. To investigate if either of the two mechanisms is more favorable, it would be interesting to study proteins of different crystallization rates.

Through literature search during the course of this project, no structures previously solved using on-chip dry-co-crystallization with SSX were found. Furthermore, no studies using on-chip crystallization on the silicon nitride membranes from Silson, which were used in this project, were found. What was found was that Silson silicon nitride membranes previously have been used with SSX using microcrystals grown off-chip and loaded to the membranes (8; 18). Furthermore, studies using on-chip crystallization on other fixed-target supports made of silicon (9) or silicon nitride (19) were found. However, non of these used co-crystallization to produce protein-ligand bound complexes. The results of this report hence contributes to the field of SSX by showing that on-chip crystallization is possible on Silson silicon nitride membranes and that on-chip co-crystallization on the membranes can be performed with both the dry- and solution-co-crystallization techniques. It would be of high value to further investigate the use of on-chip co-crystallization as all crystal handling steps are eliminated, making the method of particular interest for fragile crystals. Furthermore, since the dry-co-crystallization technique has the potential of being partly automated, this technique could possibly be efficiently used in the drug industry for screening protein-ligands interactions.

As a final remark, since structural differences were observed between the RT- and cryo-structures of the sEH-6N4 complex, it's of relevance to determine protein structures at RT since it's closer to the physiological temperature of proteins. Interpreting the significance of the observed differences were out of the scope of this thesis, however, due to the fact that differences could be observed, it can't be ruled out that differences between RT- and cryo-structures might have important biological relevance for some proteins.

5. Conclusion

This project aimed to investigate the possibilities of using on-chip co-crystallization on silicon nitride membranes with RT-SSX, and to envision the potential of using the method within drug design and development research. Using the proof-of-concept protein sEH, on-chip co-crystallization was shown not only to be possible but also to be capable of generating well-diffracting crystals suitable for RT-SSX. A major advantage with the method is that no post-crystallization crystal handling steps are needed, in contrast to off-chip crystallization and for ligand introduction with soaking, making the method of particular interest for analyzing fragile crystals. Furthermore, co-crystallization by drying the ligand on the membranes is of great interest for the drug industry as the method has the potential of being partly automated. The method could then be used within structure-based design to screen the binding of various fragments to a target protein. However, further investigations are needed to evaluate the full capability of using the method in drug design and development research, by for example studying crystals of other space groups and ligands of other characteristics. If the method can be successfully used with many different proteins and ligands, there is a great potential of developing an efficient and valuable method for screening protein-ligand interactions using RT-SSX in the drug industry.

References

[1] Öster L, Tapani S, Xue Y, Käck H. Successful generation of structural information for fragment-based drug discovery. Drug discovery today. 2015 9;20(9):1104-11.

[2] Protein Data Bank. PDB Data Distribution by Experimental Method and Molecular Type; 2022. Available from: `https://www.rcsb.org/stats/summary`.

[3] Rhodes G. Crystallography made crystal clear: a guide for users of macromolecular models. 3rd ed. Elsevier; 2010.

[4] Fischer M. Macromolecular room temperature crystallography. Quarterly Reviews of Biophysics. 2021 1;54:e1. Available from: `https://www.cambridge.org/core/product/identifier/S0033583520000128/type/journal_article`.

[5] Liu W, Wacker D, Gati C, Han GW, James D, Wang D, et al. Serial femtosecond crystallography of G protein-coupled receptors. Science (New York, NY). 2013 12;342(6165):1521-4.

[6] Kang Y, Zhou XE, Gao X, He Y, Liu W, Ishchenko A, et al. Crystal structure of rhodopsin bound to arrestin by femtosecond X-ray laser. Nature. 2015;523(7562):561-7. Available from: `https://doi.org/10.1038/nature14656`.

[7] Grünbein ML, Nass Kovacs G. Sample delivery for serial crystallography at free-electron lasers and synchrotrons. Acta Crystallographica Section D. 2019 2;75(2):178-91. Available from: `https://doi.org/10.1107/S205979831801567X`.

[8] Shilova A, Lebrette H, Aurelius O, Nan J, Welin M, Kovacic R, et al. Current status and future opportunities for serial crystallography at MAX IV Laboratory. Journal of Synchrotron Radiation. 2020 9;27(5):1095-102. Available from: `https://doi.org/10.1107/S1600577520008735`.

[9] Lieske J, Cerv M, Kreida S, Komadina D, Fischer J, Barthelmess M, et al. On-chip crystallization for serial crystallography experiments and on-chip ligand-binding studies. IUCrJ. 2019 7;6(4):714-28. Available from: `https://doi.org/10.1107/S2052252519007395`.

[10] Gelin M, Delfosse V, Allemand F, Hoh F, Sallaz-Damaz Y, Pirocchi M, et al. Combining 'dry' co-crystallization and in situ diffraction to facilitate ligand screening by X-ray crystallography. Acta Crystallographica Section D. 2015 8;71(8):1777-87. Available from: `https://doi.org/10.1107/S1399004715010342`.

[11] Wlodawer A, Minor W, Dauter Z, Jaskolski M. Protein crystallography for non-crystallographers, or how to get the best (but not more) from published macromolecular structures. The FEBS journal. 2008;275(1):1-21.

[12] Russo Krauss I, Merlino A, Vergara A, Sica F. An Overview of Biological Macromolecule Crystallization. International Journal of Molecular Sciences. 2013;14:11643-91.

[13] Dods R, Båth P, Arnlund D, Beyerlein KR, Nelson G, Liang M, et al. From macrocrystals to microcrystals: a strategy for membrane protein serial crystallography. Structure. 2017;25(9):1461-8.

[14] MAX IV Laboratory. Annual Report MAX IV Laboratory 2021; 2021. Available from: https://www.maxiv.lu.se/science/reports/.

[15] Shin S. New era of synchrotron radiation: fourth-generation storage ring. AAPPS Bulletin. 2021;31(1):21. Available from: https://doi.org/10.1007/s43673-021-00021-4.

[16] MAX IV Laboratory. Beamline map;. Available from: https://www.maxiv.lu.se/accelerators-beamlines/beamlines/.

[17] Martiel I, Beale JH, Karpik A, Huang CY, Vera L, Olieric N, et al. Versatile microporous polymer-based supports for serial macromolecular crystallography. Acta Crystallographica Section D. 2021 9;77(9):1153-67. Available from: https://doi.org/10.1107/S2059798321007324.

[18] Coquelle N, Brewster AS, Kapp U, Shilova A, Weinhausen B, Burghammer M, et al. Raster-scanning serial protein crystallography using micro- and nano-focused synchrotron beams. Acta Crystallographica Section D. 2015 5;71(5):1184-96. Available from: https://doi.org/10.1107/S1399004715004514.

[19] Norton-Baker B, Mehrabi P, Boger J, Schönherr R, von Stetten D, Schikora H, et al. A simple vapor-diffusion method enables protein crystallization inside the HARE serial crystallography chip. Acta Crystallographica Section D. 2021 6;77(6):820-34. Available from: https://doi.org/10.1107/S2059798321003855.

A. Production of macrocrystals used to produce seed

Macrocrystals for producing seed were grown using sitting-drop vapor-diffusion on the Cryschem M crystallization plate. Drops of 4 µL, consisting of protein and reservoir solution in a 1:1 ratio, were setup against a 500 µL reservoir solution of 34-40% w/v PEG 3,350, 0.1 M $Li_2SO_4 \bullet H_2O$ and 0.1 M Tris HCl pH 8.5. Furthermore, seeding was performed in half of the drops by streaking them with seed produced in a previous stock, using a Seeding Tool (Hampton Research, HR8-133).

Multiple crystals of around 10-60 µm in width and 100-300 µm in length were obtained in all drops where seeding was used. On the other hand, for the drops were no seeding was used, only one or a few large crystals, of up to 250 µm in width and 1600 µm in length, were obtained in the drops of 38% and 40% w/v PEG 3,350.

B. Fixed-target sample introduction at BioMAX

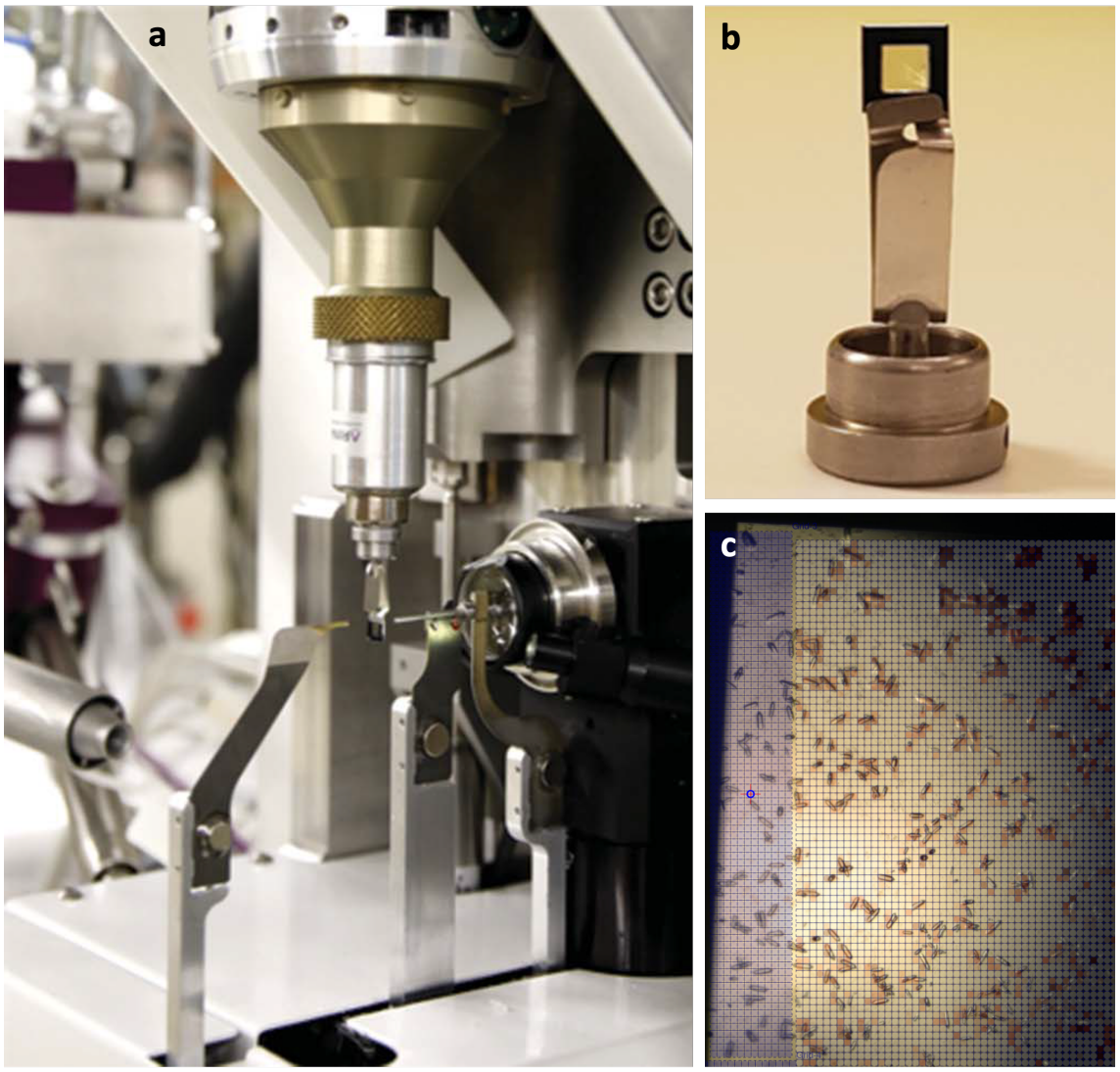

Figure B.1: Experimental set up for introducing microcrystals to the X-ray beam using fixed-target sample delivery at BioMAX. (a) Sandwiched silicon nitride membranes mounted on a goniometer head (see (b)) and placed in front of the X-ray beam. (b) Sandwiched silicon nitride membranes mounted on a goniometer head. (c) Zoomed in image of the membrane with crystals placed in front of the X-ray beam. Each grid of the membrane will be illuminated with X-rays once.

C. Drop ratio screening

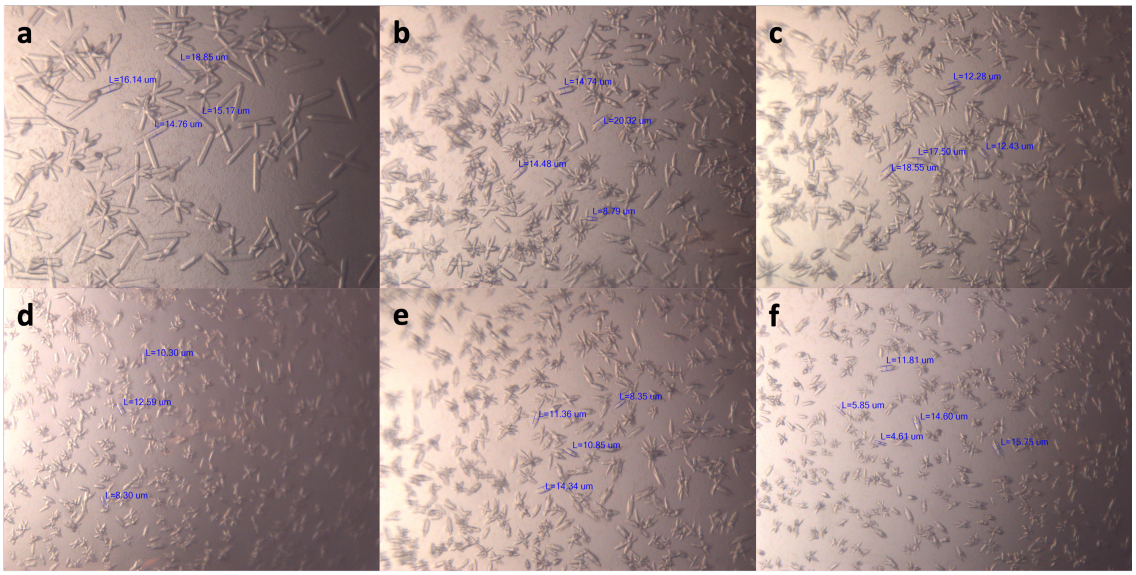

Figure C.1: Crystals grown in drops with a seed-dilution 1:128 and a protein-precipitant drop ratio of (a) 1:1, (b) 1:2, (c) 1:3, (d) 1:4, (e) 1:5, (f) 1:6.

D. Position of residue Phe497

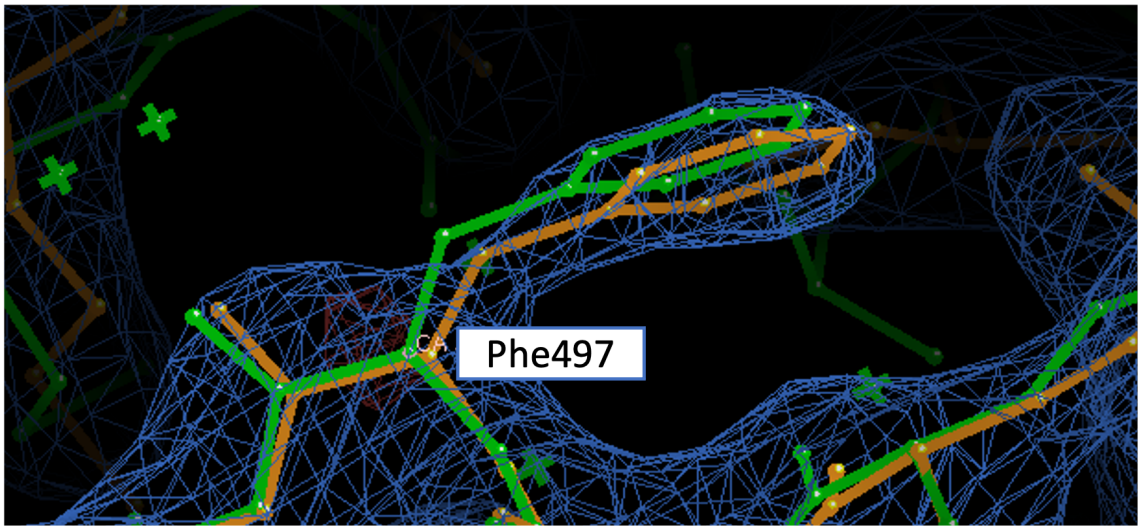

Figure D.1: Position of residue Phe497 in the RT-structure of the solution-co-crystallization samples (orange) and the cryo-structure (green). The $2F_{obs}$-F_{calc} map belongs to the RT-structure and is contoured at 1σ.

Department of Biology and Biological Engineering
Chalmers University of Technology
Gothenburg, Sweden 2022
www.chalmers.com

UNIVERSITY OF
GOTHENBURG

CHALMERS
UNIVERSITY OF TECHNOLOGY